THE JOURNAL OF BIOLOGICAL CHEMISTRY
Vol. 265, No. 15, Issue of May 25, pp. 8542-8549, 1990
Printed in U.S.A.
© 1990 by The American Society for Biochemistry and Molecular Biology, Inc.

Structural and Functional Characterization of the CD2 Immunoadhesion Domain

EVIDENCE FOR INCLUSION OF CD2 IN AN α-β PROTEIN FOLDING CLASS*

(Received for publication, December 11, 1989)

Michael A. Recny‡§¶||, Edith A. Neidhardt¶, Peter H. Sayre‡, Thomas L. Ciardelli, and Ellis L. Reinherz‡ ‡‡**

*From the ‡Laboratory of Immunobiology, Dana-Farber Cancer Institute, Departments of ‡‡Medicine and §Biological Chemistry and Molecular Pharmacology, Harvard Medical School and **Department of Pharmacology and Toxicology, Dartmouth Medical School, and ¶Procept, Inc., Cambridge, Massachusetts 02139*

The T-lymphocyte transmembrane glycoprotein CD2 plays an important physiological role in facilitating adhesion between T-lymphocytes and their cognate cellular partners. This interaction is mediated by binding of CD2 to the broadly distributed surface polypeptide LFA-3 and augments the recognition function of the CD3-Ti antigen-major histocompatibility complex receptor via stabilization of conjugate formation between cells. To define better the structural components of the CD2 extracellular region which are important in contact-mediated cellular adhesion, a single-domain CD2 immunoadhesion protein has been prepared from papain digestion of a soluble two-domain CD2 molecule. This amino-terminal domain fragment binds to LFA-3 on human B-cells with a dissociation constant of 0.4 μM, possesses functional immunoadhesion epitopes as defined by the binding of monoclonal antibodies raised to native CD2, and retains the ability to inhibit sheep erythrocyte rosette formation with human T-cells. Thus, all of the immunoadhesion functions ascribed to CD2 reside within the amino-terminal domain. Circular dichroism analysis of the isolated CD2 adhesion domain suggests the presence of substantial α-helical character (22%), consistent with earlier computer modeling analyses that predicted a pattern of alternating α-helices and β-sheets within the extracellular region of CD2. Despite the existence of short stretches of sequence homology between CD2 and immunoglobulin superfamily members, the circular dichroism data provide supporting biophysical evidence for classification of CD2 in an α-β (either α/β or $\alpha + \beta$) protein folding class.

The human CD2 surface structure is a 50-55-kDa transmembrane glycoprotein found on a vast majority of thymocytes and virtually all peripheral T-lymphocytes and is involved in mediating cellular adhesion between T-cells and their cognate partners through an interaction with the surface-bound ligand LFA-3 (Shaw *et al.*, 1986; Selveraj *et al.*, 1987; reviewed in Moingeon *et al.*, 1989a). CD2 was first identified based on the observation that T-lymphocytes form rosettes with sheep erythrocytes via CD2 interaction with T11TS, the sheep homologue of human LFA-3 (Howard *et al.*, 1981; Kamoun *et al.*, 1981; Hunig *et al.*, 1986). This interaction could be disrupted by monoclonal antibodies directed against a CD2 surface epitope defined as $T11_1$, the sheep red blood cell (SRBC)[1]-binding site (Meuer *et al.*, 1984). In contrast, monoclonal antibodies recognizing two other distinct CD2 surface epitopes (termed $T11_2$ and $T11_3$) did not block rosetting but in combination triggered antigen-independent T-cell activation (Meuer *et al.*, 1984). These results, combined with other studies, demonstrated that CD2 also plays an important role in signal transduction in T-lymphocytes. Perturbation of the CD2 extracellular domains with anti-$T11_2$ plus anti-$T11_3$ antibodies induces polyclonal T-cell activation and proliferation, secretion of interleukin-2 and surface expression of interleukin-2 receptors, and in the case of cytolytic T-lymphocytes, cytolytic effector functions (Siliciano *et al.*, 1985; Hunig *et al.*, 1987; Alcover *et al.*, 1988). It has also been shown that CD2-mediated adhesion plays an important role in augmenting the antigen recognition function of T-cells via the CD3-Ti antigen-major histocompatibility complex receptor by facilitating cell-cell conjugate formation (Yang *et al.*, 1986; Alcover *et al.*, 1987; Bierer *et al.*, 1988; Moingeon *et al.*, 1989b).

cDNA sequences for human CD2 (Sewell *et al.*, 1986; Aruffo and Seed, 1987; Sayre *et al.*, 1987), murine CD2 (Clayton *et al.*, 1987; Sewell *et al.*, 1987), and rat CD2 (Williams *et al.*, 1987) have been cloned, and the genomic organizations of human and murine CD2 have been described (Diamond *et al.*, 1988; Lang *et al.*, 1988). The human CD2 gene contains five exons spanning 12 kilobases. A leader exon contains the 5′-untranslated region and most of the nucleotides defining the signal peptide (residues −24 to −5). Two exons encode the extracellular segment; exon 2 is 321 base pairs long and codes for 4 residues of the leader peptide and residues 1-103 of the mature protein, and exon 3 is 231 base pairs long and encodes residues 104-180. Exon 4 is 123 base pairs long and codes for the single transmembrane region of the molecule (residues 181-221). Exon 5 is a large 765-base pair exon encoding virtually the entire cytoplasmic domain rich in proline and basic amino acids (residues 222-327) and the 3′-untranslated region. Murine CD2 has essentially identical intron-exon boundaries compared with human CD2, although on a protein level the two gene products share only 50% overall amino acid sequence identity (Clayton *et al.*, 1987). Substantial conser-

* This work was supported in part by National Institutes of Health Grant AI2126. The costs of publication of this article were defrayed in part by the payment of page charges. This article must therefore be hereby marked "*advertisement*" in accordance with 18 U.S.C. Section 1734 solely to indicate this fact.

|| Present address: Dept. of Protein Biochemistry, Procept, Inc., 840 Memorial Dr., Cambridge, MA 02139.

[1] The abbreviations used are: SRBC, sheep red blood cells; PBS, phosphate-buffered saline; ELISA, enzyme-linked immunosorbent assay; HPLC, high performance liquid chromatography; SDS, sodium dodecyl sulfate; PAGE, polyacrylamide gel electrophoresis.

Downloaded from www.jbc.org by guest, on December 26, 2009

vation of nucleotide sequences within both the 5′ and 3′ gene-flanking regions of human and murine CD2 suggests that both genes may be regulated in a similar fashion (Diamond *et al.*, 1988; Lang *et al.*, 1988).

Based on the genomic organization of CD2 the extracellular sequence can be divided into two polypeptide domains: residues 1–103 and residues 104–180. Accordingly, a soluble two-domain CD2 molecule ($T11_{ex2}$) comprised of all 180 residues of the extracellular sequence and 2 residues of the putative transmembrane region has been produced in a baculovirus expression system (Sayre *et al.*, 1989). This monomeric two-domain polypeptide binds directly to its cellular ligand LFA-3 with a dissociation constant of 0.4 μM and retains functional surface epitopes defined by the binding of various anti-CD2 monoclonal antibodies that recognize native CD2. Previous computer modeling analysis of the CD2 polypeptide sequence predicted a combination of alternating α-helices and β-sheet structures for the extracellular segments (Clayton *et al.*, 1987). Circular dichroism studies performed on $T11_{ex2}$ also indicated the presence of significant α-helical character in the two-domain molecule (Sayre *et al.*, 1989), providing supporting evidence for inclusion of CD2 in an α-β protein folding class (defined as either α/β or α + β; Manavalan and Johnson, 1983). However, others have argued for inclusion of CD2 in the immunoglobulin gene superfamily, based on a comparison of primary sequence homologies of CD2 with immunoglobulin κ-chain variable region hypervariable sequences (Peterson and Seed, 1987), human CD4 domains I and IV (Williams *et al.*, 1987) and other nonimmunoglobulin members of the immunoglobulin gene superfamily (Williams and Barclay, 1988). If the adhesion domain of CD2 adopts a conformation similar to a classical immunoglobulin β-fold, there should be no α-helices present within this extracellular domain.

To explore this question further and define better the external domains of CD2 which are involved in contact-mediated cellular adhesion, a single-domain CD2 immunoadhesion molecule derived from papain digestion of two-domain $T11_{ex2}$ has been purified and characterized. This amino-terminal domain fragment (T11pap) contains the functional immunoadhesion epitopes defined by the binding of various anti-CD2 monoclonal antibodies, binds to its cellular ligand LFA-3, and inhibits SRBC rosetting with human T-lymphocytes at micromolar concentrations. Thus, the immunoadhesion properties of one-domain T11pap are indistinguishable from two-domain $T11_{ex2}$. Biophysical evidence provided by circular dichroism analysis of T11pap clearly supports earlier modeling predictions that argue for classifying the external immunoadhesion domain of CD2 in an α-β protein folding class.

EXPERIMENTAL PROCEDURES

Production and Purification of Recombinant TII_{ex2} and $T4_{ex1}$—The secreted forms of soluble CD2 ($T11_{ex2}$) and CD4 ($T4_{ex1}$) comprising the entire extracellular segments of each receptor were prepared in a baculovirus expression system as described previously (Hussey *et al.*, 1988; Sayre *et al.*, 1989). Milligram quantities of soluble $T11_{ex2}$ and $T4_{ex1}$ were purified from supernatants of infected SF9 insect cells by immunoaffinity chromatography on an anti-$T11_1$ (3T48B5) monoclonal antibody column and an anti-CD4 (19Thy5D7) monoclonal antibody column, respectively. Antibodies were coupled to Affi-Gel 10 (Bio-Rad) at a concentration of 10 mg of antibody/ml of Affi-Gel 10 resin and equilibrated in 20 mM Tris-HCl, pH 6.8. Nonspecific protein was washed off of the column with 0.1 M glycine HCl, pH 5.0. Protein samples were eluted with 0.1 M glycine HCl, pH 2.0, neutralized with 1.0 M Tris-HCl, pH 8.0, concentrated using an Amicon Centrican-10 membrane, and dialyzed into phosphate-buffered saline (PBS) for structural and functional assays.

Anti-$T11_1$: Anti-$T11_2$ ELISA—Two different monoclonal antibodies that react with distinct epitopes on native CD2 (Meuer *et al.*, 1984) were utilized in a sandwich ELISA format to quantitate soluble $T11_{ex2}$ and T11pap. Ninety-six-well microtiter plates were coated with 100 μl of anti-$T11_1$ monoclonal antibody (3T48B5)/well (6 μg/ml in PBS) and incubated overnight at 25 °C. Plates were blocked with 300 μl of 20 mg/ml bovine serum albumin in PBS, 0.05% Tween 20, 0.05% thimerosal PBS/0.05% Tween 20/0.05% thimerosol (wash buffer) for 2 h at room temperature and rinsed three times with 300 μl of PBS/0.05% Tween 20/0.05% thimerosol (wash buffer). One hundred microliters of $T11_{ex2}$ standard (10–100 ng/ml) or unknown sample diluted in PBS, 0.05% Tween 20 containing 20 mg/ml bovine serum albumin was added and incubated for 2 h at 37 °C. Plates were rinsed three times with wash buffer, and 100 μl of anti-$T11_2$ monoclonal antibody (1OLD2C1) conjugated to horseradish peroxidase (160 ng/ml horseradish peroxidase conjugate) was added for 2 h at 37 °C. Plates were then rinsed four times with wash buffer and color developed by adding 100 μl of freshly prepared OPD substrate solution/well (2 mg/ml *ortho*-phenylenediamine dihydrochloride, 0.02% hydrogen peroxide, 17 mM citrate, 65 mM Na_2HPO_4). Colorimetric development was terminated after 20 min by the addition of 50 μl of 2 N sulfuric acid and the optical density recorded at 492 nm.

Peptide Synthesis, Amino Acid Composition, and NH_2-terminal Sequence Analysis—Synthetic peptides corresponding to $T11_{ex2}$ amino acid residues 33–54 (Ile-Lys-Trp-Glu-Lys-Thr-Ser-Asp-Lys-Lys-Lys-Ile-Ala-Gln-Phe-Arg-Lys-Glu-Lys-Glu-Thr-Phe), residues 45–74 (Ala-Gln-Phe-Arg-Lys-Glu-Lys-Glu-Thr-Phe-Lys-Glu-Lys-Asp-Thr-Tyr-Lys-Leu-Phe-Lys-Asn-Gly-Thr-Leu-Lys-Ile-Lys-His-Leu-Lys), and residues 78–100 (Gln-Asp-Ile-Tyr-Lys-Val-Ser-Ile-Tyr-Asp-Thr-Lys-Gly-Lys-Asn-Val-Leu-Glu-Lys-Ile-Phe-Asp-Leu) were synthesized from f-*moc* derivatives on an Applied Biosystems model 430A peptide synthesizer and deblocked in 95% trifluoroacetic acid, 2% ethanedithiol, 3% anisol for 90 min. Peptides were precipitated with cold ether, redissolved in 6 M GdnHCl, and purified by reverse phase HPLC on a Waters Deltapak semipreparative C-18 column (7.8 × 300 mm) using a gradient of acetonitrile in 0.1% trifluoroacetic acid/water. The purity of the synthetic peptides was confirmed by both amino acid analysis and amino-terminal sequencing using an Applied Biosystems 470A sequenator/120A phenylthiohydantoin analyzer. Molar concentrations of synthetic peptides, purified $T11_{ex2}$, T11pap, and $T4_{ex1}$ were determined by quantitative amino acid analysis using precolumn phenylthiocarbamyl derivatization and separation of the phenylthiocarbamyl derivatives by reverse phase HPLC.

Papain Digestions—Five milligrams of purified $T11_{ex2}$ in PBS, 10 mM dithiothreitol was digested with 22 μg of papain (Boehringer Mannheim, 21 units/mg) in a final volume of 4.5 ml at 30 °C. Ten-microgram aliquots were removed at 5, 10, and 20 min, quenched by boiling for 2 min in 2 × Laemmli SDS sample buffer, and analyzed on 15% SDS-PAGE minigels. The remaining papain-digested sample was quenched by the addition of 50 μl of iodoacetamide (2 M stock solution in methanol, prepared fresh) and passed over an anti-$T11_1$ monoclonal antibody column (3T48B5) equilibrated in 20 mM Tris-HCl, pH 6.8. Nonspecific protein was washed off of the column with 0.1 M glycine HCl, pH 5, buffer. Bound protein (T11pap) was eluted with 0.1 M glycine, pH 2.0, concentrated using an Amicon Centrprep 3 concentrator, and dialyzed into PBS for functional studies.

Circular Dichroism—Far UV CD spectra were obtained on a Jobin Yvon Mark 5 Circular Dichrograph (Instruments SA, Inc., Metuchen, NJ) calibrated with (+) 10-camphorsulfonic acid. Measurements were taken at 25, 50, and 80 °C ± 0.1 °C in 20 mM sodium phosphate, pH 7.1, in a 1-mm cell. Each spectrum represents the average of between 4 and 15 spectra taken at 0.5-nm intervals using either a 5- or 10-s response time. All spectra have been corrected by subtraction of buffer blank. Protein concentrations were determined by UV absorption at 280 nm using the following empirically derived molar extinction coefficients (1.0 mg/ml solution in PBS measured at 280 nm in a 1-cm path): $T11_{ex2}$ = 1.5, T11pap = 1.9.

Rosette Inhibition Assays—Human T-leukemic cells (Jurkat) were washed twice in semi-modified Eagle's medium, 2% fetal calf serum and resuspended at 2.5×10^6/ml. SRBC were washed twice in Hanks' buffered salt solution and resuspended at 5% (v/v). Twenty microliters of SRBC was placed in duplicate 12 × 75-mm plastic tubes and preincubated with 20 μl of semi-modified Eagle's medium, 2% fetal calf serum (control samples), $T11_{ex2}$ (0.30–30 μM), T11pap (0.30–30.0 μM), or $T4_{ex1}$ (30 μM) for 60 min at 4 °C. Subsequently, 20 ml of Jurkat (5×10^5 cells) was added. After incubating for 5 min at 37 °C, tubes were centrifuged for 5 min at 800 rpm followed by incubation for 60 min at 4 °C. The cell pellet was gently resuspended by agitation

Downloaded from www.jbc.org by guest, on December 26, 2009

and rosette formation assessed under a Zeiss photomicroscope (50–100 T-cells/microscope field).

Radiolabeled $T11_{ex2}$-binding Assays—Purified $T11_{ex2}$ and T11pap were radioiodinated by the solid phase lactoperoxidase/glucose oxidase method (Enzymobeads; Bio-Rad) as described previously (Sayre *et al.*, 1989). The cold competition assay utilized for quantitating the binding of $T11_{ex2}$ and T11pap to a human B lymphoblastoid cell line bearing LFA-3 (JY cells) was performed as follows. JY cells were washed three times in RPMI 1640, 10% fetal calf serum and resuspended at 2×10^7/ml in the same medium. 2.5×10^6 cpm of radioiodinated $T11_{ex2}$ (50 μl at 2×10^7 cpm/nmol; 0.5 μM labeled $T11_{ex2}$) was added to 2.0×10^6 JY cells that had been previously overlayed onto 0.2 ml of a 1:5 mixture of dibutyl phthalate/dioctyl phthalate in duplicate 0.5-ml plastic microcentrifuge tubes. One hundred microliters of cold competitor containing increasing concentrations (0.06–20 μM) of unlabeled $T11_{ex2}$ or unlabeled T11pap in RPMI 1640, 10% fetal calf serum was added and the mixture incubated for 60 min at 4 °C. Cells were pelleted by centrifugation for 2 min at 15,000 × *g*, and radioactivity bound to the pelleted cells was counted. Nonspecific binding was determined by preincubation of JY cells with 50 μg/ml anti-LFA monoclonal antibody 9.2.1 (generously provided by Dr. Timothy Springer, Harvard Medical School).

RESULTS

Production and Characterization of Recombinant $T11_{ex2}$ and $T4_{ex1}$—To define better the structure/function relationships within the extracellular region of the transmembrane CD2 molecule, a soluble form of CD2 ($T11_{ex2}$) was produced using a baculovirus expression vector system (Sayre *et al.*, 1989). The cDNA construct utilized to generate $T11_{ex2}$ encodes all the amino acid residues within the secretory leader region and the first two extracellular exons, plus 2 amino acid residues from the transmembrane exon. The secreted two-domain $T11_{ex2}$ molecule contains three asparagine-linked glycosylation sites that are occupied with carbohydrate chains and 4 cysteine residues that form in two intrachain disulfide bonds (Fig. 1). Using this transient eucaryotic expression system, milligram quantities of soluble $T11_{ex2}$ have been produced and purified from the supernatants of baculovirus-infected SF9 cells by immunoaffinity chromatography on an anti-CD2 monoclonal antibody column (anti-$T11_1$). This single step routinely gives >5000-fold purification and yields quantitative recovery of approximately 1.0 mg of $T11_{ex2}$/liter of infected SF9 cells. The purity of $T11_{ex2}$ is >95% as judged by scanning densitometry of Coomassie Blue-stained SDS-PAGE gels (see Fig. 3, *lane 1*).

Quantitation of soluble $T11_{ex2}$ was accomplished using a horseradish peroxidase-based sandwich ELISA employing two different anti-CD2 monoclonal antibodies. These antibodies, termed anti-$T11_1$ and anti-$T11_2$, recognize distinct surface epitopes on native transmembrane CD2 involved in both adhesion ($T11_1$) and activation ($T11_2$) functions (Meuer *et al.*, 1984). Earlier immunoprecipitation studies demonstrated that both $T11_1$ and $T11_2$ epitopes were present on soluble $T11_{ex2}$ (Sayre *et al.*, 1989). Using these two non-cross-blocking antibodies, we developed a sensitive assay (10 ng/ml antigen) for quantitating soluble $T11_{ex2}$ during expression and purification and for determining antigen concentration in purified samples (Fig. 2). This sandwich ELISA gives a linear antigen-dependent response in formats using either anti-$T11_1$ as the capture antibody and anti-$T11_2$ as the detection antibody or anti-$T11_2$ as the capture antibody and anti-$T11_1$ as the detection antibody, although the first format gives more sensitive and reproducible results. In addition, this ELISA also provided an important means to address the structural integrity of two functionally important epitopes on smaller peptide fragments generated by protease digestion of intact $T11_{ex2}$.

Papain Digestion of $T11_{ex2}$—Incubation of native $T11_{ex2}$ with papain under nondenaturing conditions results in a rapid and progressive decrease in the molecular mass of $T11_{ex2}$ from 30 to 15 kDa as judged by SDS-PAGE (Fig. 3). Within the first 5 min of digestion, three CD2-related species are clearly visible at 28, 21, and 15 kDa. Electroblotting onto polyvinylidene difluoride membranes followed by microsequence analysis of each of these bands yielded the same unambiguous NH_2-terminal sequence corresponding to the native CD2 amino terminus (data not shown). Thus, all three bands represent carboxyl-terminal truncations of $T11_{ex2}$. Within 20 min of

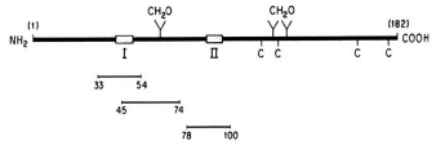

FIG. 1. **Structure of recombinant $T11_{ex2}$.** *Top,* the secreted form of soluble two-domain CD2 expressed in a baculovirus system is shown schematically. Three potential asparagine-linked glycosylation sites are illustrated (Asn^{65}, Asn^{117}, Asn^{126}), and the 4 cysteine residues (Cys^{115}, Cys^{122}, Cys^{162}, Cys^{179}) that form in two intrachain disulfide bridges are also shown. The regions of the polypeptide sequence implicated in both activation/adhesion (region I) and adhesion only (region II) are also illustrated based on previous saturation mutagenesis studies (Peterson and Seed, 1987). *Bottom,* synthetic peptides overlapping regions I and II implicated in CD2 immunoadhesion functions (residues 33–54, 45–74, and 78–100) were synthesized, purified, and tested for their ELISA reactivity and their ability to inhibit sheep erythrocyte binding to human T-cells as described under "Results."

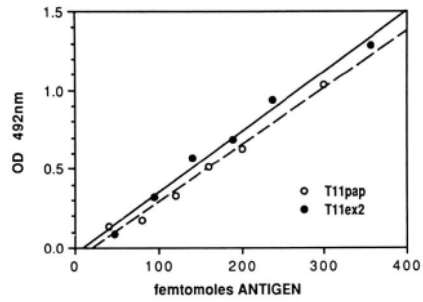

FIG. 2. **ELISA reactivity of $T11_{ex2}$ and T11pap.** Dose-response curves illustrating the molar reactivity of $T11_{ex2}$ and T11pap in the CD2 ELISA are shown. Two different anti-CD2 monoclonal antibodies were utilized in a horseradish peroxidase-based sandwich ELISA as described under "Experimental Procedures." The molar concentration of $T11_{ex2}$ and T11pap was calculated based on a polypeptide molecular mass of 21 and 12.5 kDa, respectively, and the best straight line for each dose response curve was obtained by linear regression analysis.

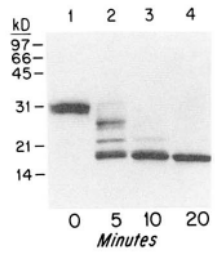

FIG. 3. **SDS-PAGE analysis of $T11_{ex2}$ and T11pap.** Samples were electrophoresed on a 15% SDS-polyacrylamide minigel as described (Laemmli, 1970), and the gel was stained with Coomassie Blue. *Lane 1,* 5 μg of native $T11_{ex2}$ purified by anti-$T11_1$ monoclonal antibody column; 5-μg aliquots of the reaction mixture showing time course digestion of native $T11_{ex2}$ with 22 ng of papain at 5 min (*lane 2*), 10 min (*lane 3*), and 20 min (*lane 4*). Molecular weight standards (Bio-Rad) were as follows: phosphorylase *b*, 97,400; bovine serum albumin, 66,200; ovalbumin, 45,000; carbonic anhydrase, 31,000; soybean trypsin inhibitor, 21,500; lysozyme, 14,400.

Downloaded from www.jbc.org by guest, on December 26, 2009

papain digestion, these bands all collapse to a stable 15-kDa species, termed T11pap. The protease-resistant T11pap fragment is stable to further digestion at longer digestion times, although at 10-fold higher enzyme concentrations, progressive degradation of this species is gradually observed.

Fig. 4 illustrates the peptide map obtained following separation of papain-digested $T11_{ex2}$ by reverse phase HPLC. T11pap corresponds to the major peak in the map, eluting at approximately 49.5 min (40% B; see legend to Fig. 4). Amino-terminal sequencing of HPLC-purified T11pap yielded 15 residues of unambiguous sequence corresponding to the mature CD2 amino terminus. Amino-terminal sequence data generated from a number of other peaks in the peptide map indicated that the vast majority correspond to peptides derived from the carboxyl-terminal half of the molecule. The major peptide eluting at 33 min yielded a sequence beginning with Lys^{108} and extending through Tyr^{115} and was the most end-proximal peptide identified in the map, suggesting that T11pap represents a proteolytically resistant, amino-terminal domain fragment corresponding roughly to the first 107 amino acid residues of $T11_{ex2}$. Based on the cDNA sequence, a polypeptide of this length would have a molecular mass of 12,616 daltons. This is in good agreement with the observed SDS-PAGE molecular weight of T11pap, since T11pap contains one glycosylation site at Asn^{65} which contains carbohydrate; digestion of T11pap with peptide *N*:glycosidase F (*N*-Glycanase) reduces the molecular mass of T11pap from 15 kDa to approximately 12 kDa as monitored by SDS-PAGE (data not shown). However, given the nonspecific nature of papain it is likely that the carboxyl terminus of T11pap is heterogeneous, spanning several residues within this protease-sensitive region. Papain digestion eliminates the two remaining asparagine-linked glycosylation sites at Asn^{122} and Asn^{126} as well as the 4 disulfide-bonded cysteine residues clustered within the second domain of $T11_{ex2}$.

Immunoaffinity purification of T11pap was accomplished by passage of the papain-digested sample over an anti-$T11_1$ monoclonal column. Starting from digestion of 5 mg of $T11_{ex2}$ (240 nmol), molar recoveries of T11pap from the immunoaffinity column were in the range of 70–80% (170–190 nmol of T11pap). To determine whether both adhesion and activation epitopes defined by anti-$T11_1$ and anti-$T11_2$ antibodies were functionally intact in this fragment, T11pap was analyzed using the CD2 sandwich ELISA (Fig. 2). Compared with $T11_{ex2}$, the single-domain T11pap molecule purified by immunoaffinity chromatography demonstrates identical immunoreactivity. ELISA analysis of T11pap purified by reverse phase HPLC also demonstrated immunoreactivity identical to $T11_{ex2}$. Thus, T11pap retains both $T11_1$ and $T11_2$ epitopes in a fully functional manner.

Binding of T11pap to Sheep Erythrocytes and Human B-Lymphoblastoid Cells—Previous biochemical characterization of soluble $T11_{ex2}$ demonstrated that micromolar concentrations of the two-domain molecule were capable of inhibiting sheep erythrocyte rosetting with Jurkat, a human leukemic T-cell line (Sayre *et al.*, 1989). Binding of $T11_{ex2}$ to its surface ligand LFA-3 expressed on a human B-lymphoblastoid cell line (JY cells) was also found to be in the micromolar range (Sayre *et al.*, 1989). To compare directly the functional properties of T11pap with $T11_{ex2}$ in ligand binding assays, the effects of T11pap on inhibition of SRBC rosetting with Jurkat cells was investigated. Fig. 5 illustrates that SRBC rosetting was inhibited in the same dose-dependent manner by both $T11_{ex2}$ and T11pap; complete inhibition of rosetting was achieved at concentrations of 10 μM for either $T11_{ex2}$ or T11pap, with half-maximal inhibition of rosetting occurring at approximately 1 μM. Control assays using $T4_{ex1}$, a soluble four-domain CD4 polypeptide also made in a baculovirus expression system (Hussey *et al.*, 1988), had no effect on SRBC binding to Jurkat cells, whereas nanomolar concentrations of anti-$T11_1$ monoclonal antibody completely abrogated SRBC rosetting with Jurkat cells.

Since T11pap clearly inhibits the interaction of human T-cells with sheep erythrocytes bearing the LFA-3 homologue T11TS, we examined whether T11pap could compete with $T11_{ex2}$ for binding to surface-bound LFA-3 on a human B-lymphoblastoid cell line. Fig. 6 shows the results obtained from a competitive binding study whereby increasing amounts of cold ligand (either $T11_{ex2}$ or T11pap) were used to compete with a constant amount of ^{125}I-radiolabeled $T11_{ex2}$ for binding to a fixed number of JY cells. Binding of ^{125}I-radiolabeled $T11_{ex2}$ is progressively inhibited by increasing concentrations of both $T11_{ex2}$ and T11pap in a dose-dependent manner; in fact, the inhibition curves are virtually identical. Half-maximal inhibition of specific binding occurs at 12,000 cpm, consistent with a IC_{50} of 0.4 μM for both $T11_{ex2}$ and T11pap. This value is in excellent agreement with the dissociation constant determined previously for the $T11_{ex2}$-LFA-3 receptor-ligand pair (Sayre *et al.*, 1989). As a control example, soluble CD4 ($T4_{ex1}$) has no effect on the binding of ^{125}I-radiolabeled $T11_{ex2}$ to JY cells.

Several attempts were made to demonstrate specific saturable binding of ^{125}I-radiolabeled T11pap to JY cells. However,

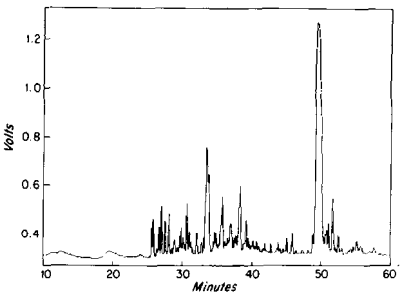

FIG. 4. **Reverse phase HPLC peptide map of papain digested $T11_{ex2}$.** One hundred micrograms of $T11_{ex2}$ was digested with papain as described under "Experimental Procedures," diluted with an equal volume of 0.1% trifluoroacetic acid/water, and injected onto a Waters Deltapak C-4 reverse phase HPLC column (3.9 × 150 mm) equilibrated in 95% A (0.1% trifluoroacetic acid/water), 5% B (0.1% trifluoroacetic acid, 90% acetonitrile, 10% water) at a flow rate of 1.0 ml/min. At 10 min, a linear gradient from 5% B to 60% B at 1%/min was initiated. Absorbance was monitored at 214 nm, and peak fractions were collected for subsequent analysis.

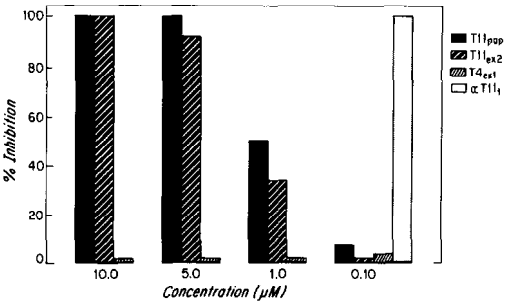

FIG. 5. **Inhibition of sheep erythrocyte rosette formation with human T-cells using soluble $T11_{ex2}$ or T11pap.** Sheep red blood cells were incubated with varying concentrations of $T11_{ex2}$, T11pap, $T4_{ex1}$, and anti-$T11_1$ monoclonal antibody (3T48B5) as described under "Experimental Procedures." The percentage of T-cell/SRBC rosettes was calculated based on comparison with control samples with media wash alone. Samples indicated as 100% inhibition showed no rosettes. For quantitation purposes, at least 150 Jurkat cells were examined/assay sample.

Downloaded from www.jbc.org by guest, on December 26, 2009

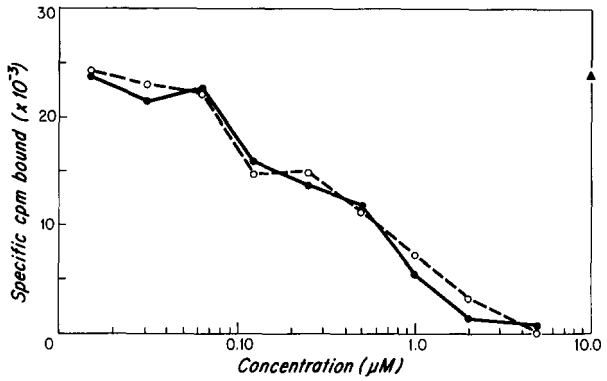

FIG. 6. **Competitive inhibition of radioiodinated $T11_{ex2}$ binding to human B-lymphoblastoid cells.** Radioiodinated $T11_{ex2}$ was added to 2.0×10^6 JY cells overlayed onto a 1:5 mixture of dibutyl phthalate/dioctyl phthalate in duplicate 0.5-ml plastic microcentrifuge tubes, as described under "Experimental Procedures." Aliquots of cold competitor containing increasing concentrations of either unlabeled $T11_{ex2}$ (*closed circles*) or unlabeled T11pap (*open circles*) were added and the mixture incubated for 60 min at 4 °C. Cells were pelleted by centrifugation, and radioactivity bound to the pelleted cells was determined. Nonspecific binding was determined by preincubation of JY cells with anti-LFA-3 monoclonal antibody 9.2.1. Specific cpm are determined by the total cpm minus cpm bound in the presence of anti-LFA-3 antibody (14,400 cpm). Specific binding in the presence of 10 μM $T4_{ex1}$ as a control is also shown (*triangle*).

using the same reaction conditions employed for successful radioiodination of $T11_{ex2}$ as judged by Scatchard analysis of specific $T11_{ex2}$ binding to JY cells (data not shown), radiolabeling of T11pap failed to result in sufficient incorporation of ^{125}I into the single-domain molecule to perform saturable binding experiments. On a molar basis, $T11_{ex2}$ routinely incorporated between 10- and 100-fold greater radioactivity than T11pap. Although 3 of the 4 predicted tyrosine residues in the extracellular segment reside within the first 86 amino acid residues of CD2, they must be relatively inaccessible to radioiodination compared with the tyrosine at residue 135 which is unique to the carboxyl-terminal domain of $T11_{ex2}$. Given the resistance of the amino-terminal adhesion domain to digestion with a relatively nonspecific protease such as papain, this result is not entirely unexpected and supports the notion of T11pap as a compact, tightly folded protein domain.

Synthetic Peptide Studies—The above results unequivocally defined the CD2 adhesion properties to reside within the T11pap protein domain. Next, we attempted to define whether there was a smaller peptide or protein fragment within T11pap which would confer all or part of the functional properties of the CD2 immunoadhesion receptor. Previous saturation mutagenesis studies identified three distinct regions within the extracellular domains of CD2 which appeared to be involved in both immunoadhesion and T-cell activation functions (Peterson and Seed, 1987). Substitutions in the CD2 polypeptide sequence centered at or about Lys^{43} (region I) dramatically reduced the ability of human erythrocytes to rosette with COS cells transfected with the mutant CD2 proteins. Amino acid mutations within region I also inhibited the binding of several CD2 antibodies that, in conjunction with a $T11_3$-like antibody, are capable of activating resting T-cells. Most of the antibodies mapped to this region also inhibit SRBC rosetting, suggesting that region I is probably involved in both activation and adhesion functions. Mutations within region II, centered at or about Gly^{90}, also significantly reduced human erythrocyte rosetting with COS cells expressing these sequence variants. Region II mutants displayed a loss of immunoreactivity with a panel of T11 antibodies that normally block SRBC rosetting but have little effect on T-cell activation. Region III was identified by a double substitution at Tyr^{135}-Gln^{136} which abrogated the binding of $T11_3$-like antibodies that are capable of triggering T-cell activation but do not block adhesion.

Thus, we synthesized three overlapping synthetic peptides corresponding to regions of the polypeptide backbone implicated in both activation/adhesion (region I) and adhesion only (region II) functions (Fig. 1, *bottom*). The peptide corresponding to residues 33–54 spans all of region I, the activation/adhesion epitope. The peptide spanning residues 45–74 covers part of the same activation/adhesion epitope and contains the single asparagine-linked glycosylation site presumed to be surface exposed; the peptide spanning residues 78–100 encompasses region II, the predicted $T11_1$ adhesion epitope. Each of the synthetic peptides was tested individually and in combination with the other peptides for their ability to block sheep erythrocyte rosetting with human T-cells. Even at peptide concentrations as high as 500 μM, no inhibition of SRBC rosetting with Jurkat cells was observed for any of the individual peptides or in multiple combinations thereof, including all three synthetic peptides together in the same assay. In addition, none of these synthetic peptides was capable of inhibiting the binding of either anti-$T11_1$ or anti-$T11_2$ antibodies to $T11_{ex2}$ in our sandwich ELISA. Competition assays using a 10^3-fold M excess of synthetic peptides over $T11_{ex2}$ showed no differences in the standard curves for detecting $T11_{ex2}$ antigen (results not shown). Apparently, these peptides do not assume solution conformations indicative of native CD2 surface epitopes and thus are not recognized by anti-$T11_1$ and anti-$T11_2$ antibodies. Alternatively, the residues encompassed within these synthetic peptides do not define directly contact sites for binding of monoclonal antibodies, as suggested by the saturation mutagenesis studies.

Circular Dichroism Analysis of T11pap—Based on the protein sequence deduced from the cDNAs of human and murine CD2, earlier predictions of secondary structure within the external domains of CD2 suggested that the extracellular segments may belong to an α-β protein folding class (Clayton *et al.*, 1987). Circular dichroism studies performed on the two-domain $T11_{ex2}$ molecule also suggested the presence of the substantial α-helical character (Sayre *et al.*, 1989). However, both domains I and II of $T11_{ex2}$ have also been proposed to adopt immunoglobulin-like structures (*i.e.* β-barrel conformations) based principally on short stretches of primary sequence homology with other members of the immunoglobulin superfamily (Williams *et al.*, 1987; Peterson and Seed, 1987; Williams and Barclay, 1988). Given the observations herein that all of the functional adhesion properties of the CD2 extracellular segment reside within the first domain defined as T11pap, we used circular dichroism analysis to obtain secondary structure information on the single domain CD2 molecule. These data would provide additional evidence to help define conformational structure within the isolated adhesion domain and address the earlier predictions favoring inclusion of CD2 in the immunoglobulin superfamily.

Fig. 7*A* compares the circular dichroism spectra of native $T11_{ex2}$ and native T11pap at equivalent molar concentrations of each molecule in the far ultraviolet region. The spectra for $T11_{ex2}$, in agreement with earlier findings (Sayre *et al.*, 1989), shows a positive absorption maximum at 198 nM, a negative minimum at 215 nm, and a slight shoulder at 225 nm. The spectra for T11pap is noticeably different; the negative minimum is substantially decreased and shifted to 213 nm, and the shoulder at 225 nm is significantly enhanced. At 50 °C, T11pap secondary structure remains intact, but conforma-

Downloaded from www.jbc.org by guest, on December 26, 2009

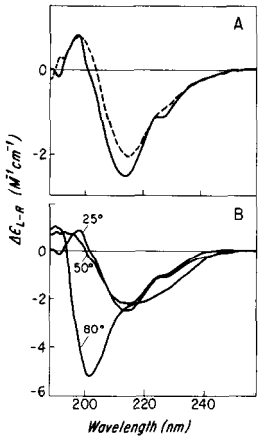

FIG. 7. **Far UV circular dichroism spectra of $T11_{ex2}$ and T11pap.** Each spectrum represents the average of between 4 and 15 individual spectra taken at 0.5-nm intervals in 20 mM sodium phosphate, pH 7.2, and corrected for background absorbance of buffer blank. Equivalent molar concentrations (30 μM) of each sample were examined. Panel *A*, CD spectra at 25 °C of $T11_{ex2}$ (– – –) and T11pap (——). *Panel B*, thermal denaturation spectra of T11pap measured at 25, 50, and 80 °C.

TABLE I

Prediction of protein secondary structure in $T11_{ex2}$ and T11pap by circular dichroism analysis

The CD data shown in Fig. 4 were analyzed for secondary structure using an updated algorithm that includes variable selection (Ahmed *et al.*, 1985) as described (Hurle *et al.*, 1987). Using this method, data for T11pap (1.05 > total % > 0.95, RMS error < 0.220), and $T11_{ex2}$ (1.03 > total % > 0.97, RMS error < 0.200) were utilized to calculate average percentages of each structural element in the samples.

Structural element	Structure	
	$T11_{ex2}$	T11pap
	%	
α-Helix	16	22
β-Sheet	21	22
Antiparallel β-sheet	7	5
Turn	16	18
Other	42	36

tional stability is lost upon heating of the single-domain molecule to 80 °C (Fig. 7*B*).

The digitized circular dichroism data were analyzed for secondary structure by an updated algorithm of a method published previously (Hennessey and Johnson, 1981), which is modified by a statistical technique called variable selection (Ahmed *et al.*, 1985). The criteria used to select the best predictions for total secondary structures from those generated by variable selection were as follows (Hurle *et al.*, 1987). (*a*) The sum of all fractions for predicted secondary structures must be in the range of 0.95–1.05; (*b*) no single fraction should have a value less than zero; and (*c*) the sum of squares of the residuals between the reconstituted CD spectrum and the observed CD spectrum (RMS error) must be less than 0.220. These results, illustrated in Table I, indicate that the percentage of α-helix calculated for the single domain T11pap molecule is significant (22%). Moreover, the overall percentage of predicted helical structures in T11pap is enhanced over that found in $T11_{ex2}$ (16%) at the expense of random coil structures. The remaining percentages of β-sheet, antiparallel β-sheet, and turn structures remain relatively constant for both T11pap and $T11_{ex2}$. These data are in good agreement with earlier computer modeling analyses of CD2 which predicted a significant percentage of α-helical structure within the amino-terminal domain of CD2, particularly within the first 25 amino acid residues (Clayton *et al.*, 1987).

DISCUSSION

We have demonstrated that a single-domain CD2 polypeptide consisting of approximately the first 107 amino acids of the extracellular sequence can be generated by papain digestion of the recombinant two-domain $T11_{ex2}$ molecule. This truncated CD2 receptor binds to its physiological ligand LFA-3 with a dissociation constant of approximately 0.4 μM based on the half-maximal inhibition point for T11pap displacement of $T11_{ex2}$ binding to JY cells. This binding affinity is essentially identical to that of $T11_{ex2}$ binding to LFA-3, based on previous results obtained with the two-domain molecule (Sayre *et al.*, 1989). Therefore, the relative binding affinities of the one- and two-domain CD2s for LFA-3 are equivalent. Consistent with the IC_{50} measurements, micromolar concentrations of this proteolytically resistant T11pap domain are also capable of completely inhibiting sheep erythrocyte rosette formation with human T-cells. Thus, binding of soluble T11pap to the sheep LFA-3 homologue T11TS directly prevents cell-cell contact presumably through the inhibition of normal receptor-ligand interactions. In addition, T11pap has been shown to retain fully reactive $T11_1$ and $T11_2$ epitopes as judged by the CD2 ELISA using monoclonal antibodies raised against native CD2 surface structures implicated in both T-cell activation and adhesion functions (Meuer *et al.*, 1984).

These results demonstrate that all of the immunoadhesion properties ascribable to surface-bound CD2 lie within the first extracellular domain of this type I integral membrane receptor, consistent with the observation that exons often code for functional domains within proteins. However, until now it was not clear what role the second extracellular domain of $T11_{ex2}$ might play in modulating the affinity of soluble two-domain $T11_{ex2}$ for LFA-3, perhaps by maintaining overall tertiary structure of the two-domain molecule or by stabilizing the CD2·LFA-3 pair itself. That T11pap is capable of binding to LFA-3 with an affinity equivalent to $T11_{ex2}$ suggests that domain II does not directly affect the immunoadhesion properties of CD2 but is required for some other functional role. Indeed, substantial evidence points to the involvement of the second extracellular domain of CD2 in antigen-independent T-cell activation via perturbation of the $T11_3$ epitope (Meuer *et al.*, 1984; Siliciano *et al.*, 1985; Alcover *et al.*, 1988). Direct evidence that signal transduction through CD2 can occur by modulation of both extracellular domains I and II comes from the observation that a combination of anti-$T11_2$ and anti-$T11_3$ monoclonal antibodies induces a series of activation events: polyphosphoinositide turnover, increase in free cytosolic calcium (Ca^{2+}), interleukin-2 gene induction and surface expression of interleukin-2 receptors, DNA synthesis, and clonal expansion (Meuer *et al.*, 1984; Siliciano *et al.*, 1985; Alcover *et al.*, 1986, 1988; Pantaleo *et al.*, 1987). The $T11_3$ activation epitope is unusual in that it is normally detected at very low levels in peripheral blood lymphocytes but can be induced within 30 min by incubating T-lymphocytes with an anti-$T11_2$ antibody (Meuer *et al.*, 1984). Saturation mutagenesis studies suggest that the $T11_3$ epitope is localized to or affected by the Tyr^{135}/Gln^{136} residue pair in domain II (Peterson and Seed, 1987), since mutating both of these residues abrogates the binding of a $T11_3$-like antibody (9.1). The $T11_3$ epitope is clearly present on soluble two-domain $T11_{ex2}$, as evidenced by the ability of $T11_{ex2}$ to inhibit the binding of anti-$T11_3$-FITC to Jurkat, which constitutively expresses the $T11_3$ epitope (results not shown). T11pap, however, cannot block the binding of anti-$T11_3$-FITC to Jurkat. The loss of

Downloaded from www.jbc.org by guest, on December 26, 2009

anti-$T11_3$ reactivity is consistent with the proteolytic removal of domain II from $T11_{ex2}$.

Attempts to design a synthetic immunoadhesion peptide that would block CD2-LFA-3 interaction proved unsuccessful. Despite information provided by mutational analysis which defined two regions of the CD2 polypeptide sequence implicated in either direct or indirect binding of CD2 to LFA-3 (Peterson and Seed, 1987), synthetic peptides spanning the predicted adhesion epitopes failed to block SRBC rosettes with Jurkat. Apparently, peptides spanning regions I and II failed to adopt solution conformations that would bind sheep LFA-3 in the same functional manner as the polypeptide sequences comprising the functional epitopes within the CD2 immunoadhesion domain. In addition, these peptides did not compete with $T11_{ex2}$ in the sandwich ELISA, which utilizes antibodies that recognize both $T11_1$ and $T11_2$ epitopes. Therefore, the protease-resistant T11pap domain is a compact, tightly folded adhesion molecule whose functional epitopes are apparently defined by multiple contact regions on the surface of the protein. Nevertheless, whether the polypeptide sequences centered about Lys^{43} and Gly^{90} represent direct contact residues for either LFA-3 or monoclonal antibody binding or important framework residues that serve to maintain a three-dimensional conformation for these activation/adhesion epitopes remains to be defined by future crystallographic analysis of the CD2 immunoadhesion domain.

Secondary structure data provided by circular dichroism analysis of T11pap predict the presence of a substantial percentage (22%) of α-helix within the amino-terminal adhesion domain of CD2. This finding confirms previous secondary structure predictions of CD2 (Clayton *et al.*, 1987), which suggested a pattern of alternating α-helices and β-strands for the external domain segments of CD2. The circular dichroism data presented here provide direct biophysical evidence for classification of the CD2 adhesion domain in an α-β protein folding class, defined as either one of two protein folding classes ($\alpha + \beta$ or α/β) that contain both α-helix and β-sheet structures (Levitt and Chothia, 1976; Manavalan and Johnson, 1983). Proteins belonging to the $\alpha + \beta$ folding class tend to have domains whereby α- and β-structures are segregated along the polypeptide chain, such as in ribonuclease (Wyckoff *et al.*, 1970; Carlisle *et al.*, 1974) and hen egg white lysozyme (Blake *et al.*, 1965; Moult *et al.*, 1976). The α/β folding class contains proteins with predominantly β-sheets in the center of the domain and α-helices surrounding them. Thus, α- and β-structures tend to alternate along the polypeptide backbone as in flavodoxin, a typical α/β-protein of known three-dimensional structure (Burnett *et al.*, 1974). However, one cannot distinguish between these two protein folding classes on the basis of circular dichroism data alone since the predicted percentages of each structural element represent an average value for the entire molecule.

Others have argued for inclusion of CD2 in the immunoglobulin gene superfamily based on comparison of primary sequence homologies of CD2 with immunoglobulin κ-chain hypervariable sequences (Peterson and Seed, 1987), human CD4 domains I and IV (Williams *et al.*, 1987), and other non-immunoglobulin members of the immunoglobulin superfamily (Williams and Barkley, 1988). However, the classic domain structure of the immunoglobulin-related fold consists of a β-barrel conformation containing seven (in constant domains) or nine (in variable domains) β-strands assembled into two antiparallel β-sheets with no α-helices present (reviewed in Amzel and Poljak, 1979; and Davies and Metzger, 1983). Nearly all members of the immunoglobulin superfamily have a conserved intradomain disulfide bridge, although some recent inclusions in the family lack this structural element (Williams and Barclay, 1988). In this regard, T11pap lacks the evolutionarily conserved disulfide loop of most immunoglobulin family members, unlike disulfided-bonded domain I of CD4 which bears the most primary sequence homology to CD2 (Williams *et al.*, 1987). Although the limited sequence homologies between CD2 and immunoglobulin variable region domains suggest that they may have been derived from a common ancestral gene, the combination of computer modeling predictions and data provided by circular dichroism analyses strongly suggests that the LFA-3-binding domain of human CD2 appears to adopt a conformational structure more characteristic of an α-β-protein rather than a classic immunoglobulin-related β-fold. The two-domain CD2 extracellular region, however, may adopt a hybrid conformation similar to major histocompatibility class I molecules (Bjorkman *et al.*, 1987) whereby the domain closest to the membrane is β-pleated, and the immunoadhesion domain is an α/β-structure oriented above.

Given that the immunoadhesion properties of CD2 are functionally present in a soluble single-domain polypeptide as defined herein by T11pap, we are pursuing the expression of a recombinant version of a single domain CD2 molecule for further structural and functional studies. The availability of a recombinant single-domain CD2 immunoadhesion molecule might also allow for crystallographic studies to define better the overall secondary structure and spatial orientation of the important regions defined by antibodies binding to multiple CD2 activation and adhesion epitopes.

Acknowledgments—We wish especially to thank Dr. Michael Concino for development of the CD2 ELISA, Amita Vaid, Ruth Steinbrich, and Maria Knoppers for excellent technical assistance, Dr. Phillipe Moigneon and Christopher Stebbins for anti-$T11_3$-fluorescein isothiocyanate antibody, Peter Lopez for fluorescence-activated cell sorting analysis, and the scientific staff at Procept, Inc. for critical review of the manuscript.

REFERENCES

Ahmed, S. A., Miles, E. W., and Davies, D. R. (1985) *J. Biol. Chem.* **260,** 3716–3718

Alcover, A., Weiss, M. J., Daly, J. F., and Reinherz, E. L. (1986) *Proc. Natl. Acad. Sci. U. S. A.* **83,** 2614–2618

Alcover, A., Ramarli, D., Richardson, N. E., Chang, H. C., and Reinherz, E. L. (1987) *Immunol. Rev.* **95,** 1–36

Alcover, A., Alberini, C., Acuto, O., Clayton, L. K., Transey, C., Spagnoli, G. L., Moingeon, P., Lopez, P., and Reinherz, E. L. (1988) *EMBO J.* **7,** 1973–1977

Amzel, L. M., and Poljak, R. J. (1979) *Annu. Rev. Biochem.* **48,** 961–997

Aruffo, A., and Seed, B. (1987) *Proc. Natl. Acad. Sci. U. S. A.* **84,** 3365–3369

Bierer, B. E., Peterson, A., Barbosa, J., Seed, B., and Burakoff, S. J. (1988) *Proc. Natl. Acad. Sci. U. S. A.* **85,** 1194–1198

Bjorkman, P. J., Saper, M. A., Sameaoui, B., Bennett, W. S., Strominger, J. L., and Wiley, D. C. (1987) *Nature* **329,** 506–512

Blake, C. C. F., Koenig, D. F., Mair, G. A., North, A. C. T., Phillips, D. C., and Sarma, V. R. (1965) *Nature* **206,** 757–763

Burnett, R. M., Darling, G. D., Kendall, D. S., LeQuesne, M. E., Mayhew, S. G., Smith, W. W., and Ludwig, M. L. (1974) *J. Biol. Chem.* **249,** 4383–4392

Carlisle, C. H., Palmer, R. A., Mazumdar, S. I. C., Gorinsky, B. A., and Yeates, D. G. R. (1974) *J. Mol. Biol.* **85,** 1–18

Clayton, L. K., Sayre, P. H., Novotny, J., and Reinherz, E. L. (1987) *Eur. J. Immunol.* **17,** 1367–1370

Davies, D. R., and Metzger, H. (1983) *Annu. Rev. Immunol.* **1,** 87–117

Diamond, D. J., Clayton, L. K., Sayre, P. H., and Reinherz, E. L. (1988) *Proc. Natl. Acad. Sci. U. S. A.* **85,** 1615–1619

Hennessey, J. P., and Johnson, W. C. (1981) *Biochemistry* **20,** 1085–1094

Howard, F. D., Ledbetter, J. A., Wong, J., Bieber, C. P., Stinson, E.

Downloaded from www.jbc.org by guest, on December 26, 2009

B., and Herzenberg, L. A. (1981) *J. Immunol.* **126,** 2117–2122
Hünig, T., Mitnacht, R., Tiefenthaler, G., Kohler, C., and Miyasaka, M. (1986) *Eur. J. Immunol.* **16,** 1615–1621
Hünig, T., Tiefenthaler, G., Meyer zum Buschenfelde, K.-H., and Meuer, S. C. (1987) *Nature* **326,** 298–301
Hurle, M. R., Matthews, C. R., Cohen, F. E., Kuntz, I. D., Toumadje, A., and Johnson, W. C. (1987) *Proteins* **2,** 210–224
Hussey, R. E., Richardson, N. E., Kowalski, M., Brown, N. R., Chang, H.-C., Siliciano, R. F., Dorfman, T., Walker, B., Sodroski, J., and Reinherz, E. L. (1988) *Nature* **331,** 78–81
Kamoun, M., Martin, P. J., Hansen, J. A., Brown, M. A., Siadak, A. W., and Nowinski, R. C. (1981) *J. Exp. Med.* **153,** 207–212
Laemmli, U. K. (1970) *Nature* **227,** 680–685
Lang, G., Wotton, D., Owen, M. J., Sewell, W. A., Brown, M. H., Mason, D. Y., Crumpton, M. J., and Kioussis, D. (1988) *EMBO J.* **7,** 1675–1682
Levitt, M., and Chothia, C. (1976) *Nature* **261,** 552–557
Manavalan, P., and Johnson, W. C., Jr. (1983) *Nature* **305,** 831–832
Meuer, S. C., Hussey, R. E., Fabbi, M., Fox, D., Acuto, O., Fitzgerald, K. A., Hodgdon, J. L., Protentis, J. P., Schlossman, S. F., and Reinherz, E. L. (1984) *Cell* **36,** 897–906
Moingeon, P., Chang, H. C., Sayre, P. S., Clayton, L. K., Alcover, A., Gardner, P., and Reinherz, E. L. (1989a) *Immunol. Rev.* **111,** 111–141
Moingeon, P., Chang, H. C., Wallner, B. P., Stebbins, C., Frey, A. Z., and Reinherz, E. L. (1989b) *Nature* **339,** 312–314
Moult, J., Yonath, A., Traub, W., Smilansky, A., Podjarny, A., Rabinovich, D., and Saya, A. (1976) *J. Mol. Biol.* **100,** 179–195
Pantaleo, G., Olive, D., Poggi, A., Kozumbo, W. J., Moretta, L., and Moretta, A. (1987) *Eur. J. Immunol.* **17,** 55–62
Peterson, A., and Seed, B. (1987) *Nature* **329,** 842–846
Sayre, P. H., Chang, H. C., Hussey, R. E., Brown, H. R., Richardson, N. E., Spagnoli, G., Clayton, L. K., and Reinherz, E. L. (1987) *Proc. Natl. Acad. Sci. U. S. A.* **84,** 2941–2945
Sayre, P. H., Hussey, R. E., Chang, H. C., Ciardelli, T. L., and Reinherz, E. L. (1989) *J. Exp. Med.* **169,** 995–1009
Selvaraj, P., Plunkett, M. L., Dustin, M., Sanders, M. E., Shaw, S., and Springer, T. A. (1987) *Nature* **326,** 400–403
Sewell, W. A., Brown, M. H., Dunne, J., Owen, M. J., and Crumpton, M. J. (1986) *Proc. Natl. Acad. Sci. U. S. A.* **83,** 8718–8722
Sewell, W. A., Brown, M. H., Owen, M. J., Funk, P. J., Kozak, C. A., and Crumpton, M. J. (1987) *Eur. J. Immunol.* **17,** 1015–1020
Shaw, S., Luce, G. E. G., Quinones, R., Gress, R. E., Springer, T. A., and Sanders, M. E. (1986) *Nature* **323,** 262–264
Siciliano, R. F., Pratt, J. C., Schmidt, R. E., Ritz, J., and Reinherz, E. L. (1985) *Nature* **317,** 428–430
Williams, A. F., and Barclay, A. N. (1988) *Annu. Rev. Immunol.* **6,** 381–402
Williams, A. F., Barclay, A. N., Clark, S. J., Patterson, D. J., and Willis, A. C. (1987) *J. Exp. Med.* **165,** 368–380
Wyckoff, H. W., Tsernoglou, D., Hanson, A. W., Knox, J. R., Lee, B., and Richards, F. M. (1970) *J. Biol. Chem.* **245,** 305–328
Yang, S. Y., Chouaib, S., and Dupont, B. O. (1986) *J. Immunol.* **137,** 1097–1100

Downloaded from www.jbc.org by guest, on December 26, 2009